Cardiovascular Research Advance Access published June 22, 2011

Segment-Specific Differences in the Inward Rectifier K^+ Current Along the Renal Interlobular Artery

Lisa Chilton[1*], Sergey V. Smirnov[2*], Kathy Loutzenhiser[3], Xuemei Wang[3], and Rodger Loutzenhiser[3]

*These authors contributed equally to this publication.

[1]School of Veterinary and Biomedical Sciences,
James Cook University,
Douglas, Queensland, 4811,
Australia.

[2] Department of Pharmacy and Pharmacology,
University of Bath,
Claverton Down, Bath, BA2 7AY,
England.

[3] Smooth Muscle Research Group,
University of Calgary Faculty of Medicine,
3330 Hospital Drive, N.W.
Calgary, Alberta, T2N 4N1,
Canada.

Address Correspondence to:
Rodger Loutzenhiser, PhD,
Smooth Muscle Research Group,
University of Calgary Faculty of Medicine,
3330 Hospital Drive NW,
Calgary, Alberta, T2N 4N1,
Canada.

phone: (403) 220-8860
fax: (403) 270-2211
email: rloutzen@ucalgary.ca

Abstract

Aims: We investigated the role of the inward rectifier K^+ channel (K_{IR}) in the renal interlobular artery (ILA). The ILA supplies the afferent arteriole and ranges in diameter from >100 µm near its origin at the arcuate artery to <30 µm at its most distal segment.

Methods and Results: Vasodilatory responses to elevated extracellular K^+ (15 mmol/L) and vasoconstrictor responses due to K_{IR} blockade by Ba^{2+} (10-100 µmol/L) were assessed in *in vitro* perfused hydronephrotic rat kidneys. The distal ILA (26±1 µm) exhibited K^+-induced dilation and Ba^{2+}-induced vasoconstriction; whereas, neither response was observed in the proximal ILA (108±3 µm). The intermediate ILA (55±1 µm) exhibited a modest K^+-induced vasodilatation, but no Ba^{2+}-induced vasoconstriction. The K^+-induced dilations were blocked by Ba^{2+}, but not by ouabain. Ba^{2+}-induced depolarization, measured in ILA segments from normal kidneys, decreased with the increasing diameter. Patch clamp studies demonstrated that the K_{IR} current (I_{KIR}) density also was inversely correlated with ILA segment diameter. Myocytes from afferent arterioles and distal ILAs exhibited similarly large I_{KIR}, whereas, this current was absent in proximal ILA myocytes. Finally, we found that Ba^{2+} attenuated myogenic vasoconstriction, suggesting an involvement of I_{KIR}. The previously shown pattern of myogenic reactivity of the ILA (distal > intermediate>proximal) mirrors the distribution of I_{KIR} reported in the present study, further supporting a role for I_{KIR}.

Conclusions: Our findings indicate differences in the magnitude of I_{KIR} along the ILA and suggest that the influence of K_{IR} on reactivity increases as vessel diameter decreases from proximal to distal regions.

Key Words: Renal Microcirculation, Smooth Muscle Cells, Potassium Channels, Patch-Clamp Technique, Interlobular Artery

Introduction:

The inward rectifier (K_{IR}) occupies a unique niche among vascular K^+ channels. These channels typically do not contribute to the membrane potential of larger conduit arteries, but are commonly expressed in resistance vessels, suggesting an important role in the regulation of blood flow and microvascular pressures. Moreover, K_{IR} is implicated in responses unique to resistance vessels. For example, elevations in interstitial K^+ elicit vasodilatation, in part, by modulating K_{IR}[1,7, 19] and this mechanism has been suggested to contribute to responses attributed to an endothelium-derived hyperpolarizing factor (EDHF) [6]. K_{IR} has been implicated in myogenic vasoconstriction and in the conduction of electrical signals along small arterioles, as membrane stress inhibits K_{IR} in cerebral vessels [34] and blockade of K_{IR} blocks conducted vasodilation[9,26,27]. Accordingly, information on the distribution of this channel is important in regard to our understanding of the integration of signals within the vasculature and the functional properties of the various segments of the vasculature.

Regional heterogeneity in the distribution of K_{IR} is seen in a number of vascular beds[25, 30] and may also exist within the kidney. Prior *et al.*[22] demonstrated that the arcuate artery, a renal conduit vessel, does not exhibit Ba^{2+}-sensitive K^+-induced vasodilatation and, while K_{IR} could be detected in a fraction of arcuate myocytes (~5%), the current density was too low to play a significant role in regulating membrane potential. By contrast, our laboratory found K_{IR} to be a major determinant of membrane potential in the renal afferent arteriole[3] and that myocytes isolated from pre-glomerular afferent and post-glomerular efferent arterioles express $K_{IR}2.1$ and exhibit Ba^{2+}-sensitive K_{IR} currents[4]. Similarly, Cao *et al.*[2] found K_{IR} to be present in the smooth muscle-like contractile pericytes that regulate the diameter of the descending vasa recta. The

interlobular artery (ILA, also known as the cortical radial artery) originates at the arcuate artery and radiates towards the surface of the kidney, terminating with the formation of the afferent arterioles. The ILA exhibits differing properties in the larger proximal versus smaller distal segments. For example, while the distal ILA exibits myogenic vasoconstriction, this property is not seen in the larger proximal segments[8, 28]. The function of K_{IR} has not previously been examined in this unique vessel, which exhibits properties of both conduit and resistance vessels along its length.

To address this issue, we studied the functional role and the distribution of K_{IR} along the ILA, using the in vitro perfused hydronephrotic rat kidney model and patch-clamp techniques. Vasoconstrictor responses to Ba^{2+} and vasodilatory responses to increases in external K^+ ($[K^+]_o$) were evaluated in proximal, intermediate and distal segments of the ILA using the hydronephrotic kidney. Whole-cell voltage-clamp studies were used to evaluate K_{IR} currents in native myocytes obtained from afferent arterioles and proximal, intermediate and distal segments of the ILA individually isolated from the normal rat kidneys. The perforated-patch technique was used to measure changes in membrane potential in individual ILA segments. Our findings reveal segment-specific variation in the role of K_{IR} along the ILA and have important implications regarding the determinants of vasomotor regulation in the renal vasculature.

Methods:

All procedures complied with University of Calgary Animal Ethics and Canadian Council on Animal Care regulations and conformed with the *Guide for the Care and Use of Laboratory Animals* published by the US National Institutes of Health (NIH Publication No. 85-23, revised 1996). The in vitro perfused hydronephrotic rat kidney was used to evaluate the effects of Ba^{2+}

and elevated $[K^+]_o$ on the ILA. Past studies demonstrate that responses in this model correspond to not only that of vessels isolated from normal kidneys, but also to the responses of normal kidneys in vitro and in vivo[4,15,16,17,29]. Unilateral hydronephrosis was induced in male Sprague Dawley rats by ligating the left ureter under halothane anesthesia. Hydronephrotic kidneys were harvested, using halothane anesthesia, after 6-8 weeks when advanced tubular atrophy allows visualization of the microvasculature. In each case, the level of anesthesia was monitored by assessing digital reflex responses. The renal artery was cannulated and the kidney excised with continuous perfusion. Perfusion pressure was monitored at the renal artery. Kidneys were allowed 1 hour to recover prior to initiation of experimental protocols. Diameters were measured by on-line image processing[3,4,15,29]. Hydronephrotic kidneys were perfused with modified Dulbecco's Minimum Eagle's Medium (DMEM, GIBCO) containing (in mmol/L) 1.6 Ca^{2+}, 30 bicarbonate, 5 glucose, 1 pyruvate and 5 HEPES. Ibuprofen (10 μmol/L) was added to eliminate the effects of renal prostanoids[29]. Elevated KCl solutions were prepared by isotonic substitution for NaCl. Ouabain was prepared fresh for each experiment (3 mmol/L). Phentolamine and propranolol (10 μmol/L) were added to the ouabain solution to avoid effects mediated by transmitter release.

K_{IR} currents (I_{KIR}) were evaluated using patch-clamp (23ºC). Renal microvessels were isolated from the renal cortex (excluding the juxtamedullary area) of normal rat kidneys using the gel-perfusion technique[17]. Diameters were estimated by a calibrated ocular reticle and ILA segments ranging from 30 to 70 microns were selected for study. Voltage-clamp studies were performed using the whole-cell configuration on native myocytes obtained from individual microvessels[4]. Borosilicate glass pipettes were pulled to a 2-3 μm tip diameter and fire polished.

Pipettes were filled with a solution containing (mmol/L): K^+-gluconate (120), KCl (20), HEPES (10), Na_2ATP (2), Na_2GTP (0.1), EGTA (5), $MgCl_2$ (2), $CaCl_2$ (0.1), pH=7.2; pipette resistance 6-12 MΩ. The free Ca^{2+} and Mg^{2+} were calculated to be 5.1 and 0.38 mmol/L [Maxchelator, http://www.stanford.edu/~cpatton/downloads.htm]. The 30 mM K^+ external bath solution contained (mmol/L): KCl (30), NaCl (110), $MgSO_4$ (1), HEPES (5), $CaCl_2$, (1.5), glucose (5.6), pH=7.35. To minimize contributions of other K^+ channels, 5 mmol/L 4-aminopyridine and 10 µmol/L glibenclamide were included in the bath solution. In whole-cell configuration, a voltage ramp protocol (-120 to +60 mV, 1 s) was applied every 5 s from a holding potential of -40 mV (pClamp, v.8). Currents were digitized at 500-µs intervals and filtered with low-pass filter at 2 KHz on-line (Axoclamp 200B amplifier; Axon Instruments, Union City, CA). Traces were outputted at 1 KHz off-line for analysis. An agar bridge (3 mol/L KCl) was used with the reference electrode. Data were not corrected for the liquid junction potential (~4 mV[33]). Membrane potentials were recorded in arterioles (32°C), using the perforated-patch method with 400 µg/ml nystatin in a pipette solution containing (mmol/L): K^+-gluconate (120), KCl (20), HEPES (10), EGTA (5), $MgCl_2$ (0.5), $CaCl_2$ (0.1), pH=7.2.

Data are expressed as the means using the standard error of the mean as an index of dispersion. Differences between means were evaluated by paired or unpaired Student's *t* test. Probabilities (*P*) of less than 0.05 were considered significant. For multiple measurements, analysis of variance (ANOVA) followed by Bonferroni *t* test were applied to assess significance.

Results:

To evaluate the functional role of K_{IR} in intact vessels we determined if elevated extracellular K^+ evoked a Ba^{2+}-sensitive and ouabain-insensitive vasodilatation and if blockade

of K_{IR} by Ba^{2+} induced a vasoconstriction. Since the ILA is tapered along its length, segments were identified based on basal diameter[8]. ILAs were selected near their origin (proximal ILA diameter 107.5±2.9 μm, n=6), at an intermediate point (intermediate ILA diameter 52.4±1.1 μm, n=5), or at their termini (distal ILA diameter 26.2±0.9 μm, n=26).

K^+-induced vasodilatation in the distal ILA

Figure 1A illustrates the effects of elevating $[K^+]_o$ on the myogenic vasoconstriction in a 21 micron (distal) segment of an ILA. Note, the vasoconstriction induced by increasing renal arterial pressure (RAP) from 80 to 160 mmHg and the vasodilation evoked by increasing $[K^+]_o$ (15 mmol/L). Returning $[K^+]_o$ to 5 mmol/L restored the vasoconstriction. Mean data are presented in Figure 1B. Increasing RAP reduced diameters from 26.2±0.9 to 17.5±1.0 μm (n=26) and 15 mmol/L KCl increased diameters to 26.3±1.2 μm (P<0.0001). In a separate series, pressure was held at 80 mmHg and tone was elevated with angiotensin II (Ang II, 0.1 nmol/L). Diameters were reduced from 21.9±0.4 to 8.2±0.8 μm (P= 0.001, n=4, Figure 1B) and 15 mmol/L $[K^+]_o$ increased diameters to 21.2±0.8 μm (P=0.001 versus Ang II alone). Returning $[K^+]_o$ to 5 mmol/L, restored the Ang II-induced vasoconstriction (7.9±0.9 μm, data not shown).

Elevations in $[K^+]_o$ may evoke hyperpolarization and vasodilatation by enhancing the outward component of I_{KIR} or by stimulating the electrogenic Na^+/K^+ ATPase pump[1,12, 19, 22]. To evaluate the contributions of these two mechanisms, we determined the effects of Ba^{2+} (100 μM) and ouabain (3 mmol/L) on the vasodilatation evoked by elevated $[K^+]_o$. In these studies, the administration of Ba^{2+} or ouabain was sufficient to establish a vasoconstriction. As shown in Figure 1B, Ba^{2+} decreased distal ILA diameters from 21.5±1.0 to 8.9±0.7 μm (n=6) and the subsequent administration of 15 mmol/L KCl failed to evoke vasodilatation (8.6±0.6 μm,

P=0.38). Ouabain reduced distal ILA diameters from 21.6±0.9 to 7.9±0.7 μm (n=11, Figure 1B). As described previously[3], to compensate for the effects of ouabain on intracellular [K^+], extracellular [K^+] was increased from 5 to10 mmol/L in these experiments. This manipulation increased diameters to 15.5±1.2 μm (*P*<0.0001). In a separate series, distal segments were treated with a combination of ouabain plus 100 μmol/L Ba^{2+}, which reduced diameters to 8.5±0.7 μm. The subsequent addition of 10 mmol/L KCl failed to significantly increase diameter (7.6±0.6 μm, *P*=0.06, n=8). Thus K^+-induced vasodilatation of the distal ILA was inhibited by Ba^{2+}, but not by ouabain, implicating the involvement of K_{IR}.

K^+-induced responses of the intermediate and proximal ILA

The intermediate ILA has less myogenic reactivity and the proximal ILA does not exhibit this response[8, 28]. For this reason, Ang II (1 nmol/L) was used to establish basal tone for these studies. Ang II reduced diameters of the intermediate ILA from 55.4±1.4 to 43.2±1.2 μm (Figure 2A, n=5). Increasing $[K^+]_o$ to 15 mmol/L increased diameters to 47.0±1.5 μm (*P*=0.0034). Diameters recovered to 42.5±0.8 μm when $[K^+]_o$ was returned to 5 mmol/L (not shown). Ouabain, administered in the presence of Ang II, had no additional effect on diameter (42.7±0.9 μm), and elevating $[K^+]_o$ (10 mmol/L) increased diameters to 47.8±1.7 μm (*P*=0.006, Figure 2A, *P*=0.18 vs control). By contrast, Ba^{2+} inhibited K^+-induced vasodilation. ILA diameters were 46.7±1.6 μm in Ba^{2+} plus Ang II and 40.3±2.8 upon addition of 15 mmol/L $[K^+]_o$ (*P*=0.14, Figure 2A). In a separate group treated with Ba^{2+}, ouabain, and Ang II, diameters were 44.4±1.6 μm in 5 mmol/L $[K^+]_o$ and 38.7±2.9 μm (*P*=0.07) in 15 mmol/L $[K^+]_o$.

In the proximal ILA, 1 nmol/L Ang II reduced diameters from 107.5±2.9 to 74.8±6.4 μm (n=6, Figure 2B). In contrast to the smaller ILA segments, rather than inducing vasodilatation, 15

mmol/L KCl caused a further constriction to 55.6±4.6 μm (n=6, *P*=0.007). Figure 2C compares the responses of the distal, intermediate and proximal ILA to elevated $[K^+]_o$. Vessel diameters are normalized to the basal diameter. Note that while a relatively modest K^+-induced dilation was observed in the intermediate ILA, this response was absent in the proximal ILA. For comparative purposes, previously published data[4] on afferent arteriolar response to elevated $[K^+]_o$ in the presence of Ang II-induced vasoconstriction are also presented.

Segmental variations in the vasoconstrictor effects of Ba^{2+} on the ILA

We next determined if blockade of K_{IR} evokes vasoconstriction in the ILA. These studies were conducted at a RAP of 40 mmHg. Under these conditions, proximal ILA diameters were 100.8±2.1 μm (n=9, Figure 3A). Following the application of 10, 30, and 100 μmol/L Ba^{2+}, diameters were 94.5±5.2 μm (*P*=0.26), 91.7±7.6 μm (*P*=0.27) and 89.4±7.7 μm (*P*=0.17), respectively. Similarly, Ba^{2+} did not constrict the intermediate ILA. Basal diameters were 51.1±1.1 μm (n=5) and diameters were 51.1±1.5 μm, 50.3±1.2 μm (*P*=0.2739) and 49.2±2.1 μm (*P*=0.2656) in 10, 30 and 100 μmol/L Ba^{2+}, respectively (Figure 3A). By contrast, Ba^{2+} elicited a concentration-dependent constriction of the distal ILA. Diameters were 20.1±0.9 μm in controls and 18.8±1.2 μm in the presence of 10 μmol/L Ba^{2+} (n=6, *P*=0.26, Figure 3C). At 30 and 100 μmol/L Ba^{2+}, diameters were reduced to 15.3±1.4 μm (*P*=0.0286) and 12.9±1.3 μm (*P*=0.0154), respectively (Figure 3A). Data summarizing the effects of Ba^{2+} on each ILA segment and, for comparative purposes, on the afferent arteriole under similar conditions [previously published[3]], are shown in Figure 3B. Diameters are normalized to the basal values for each vessel.

Figures 3C&D illustrate the differing effects of Ba^{2+} on membrane potentials of isolated vessels. As shown in the tracings (Figure 3C), 100 μmol/L Ba^{2+} evoked depolarization in the

afferent arteriole, but not in a 60 µm ILA segment. Figure 3D illustrates the significant inverse relationship between the magnitude of the Ba^{2+}-induced depolarization and diameter in 9 vessels studied using this approach.

Patch-clamp studies of myocytes from afferent arterioles and segments of the ILA

The above observations suggest an important contribution of the outward component of I_{KIR} in setting membrane potential of the afferent arteriole and distal ILA. Online Figure 1S illustrates the presence of the small outward I_{KIR} seen in afferent arteriolar myocytes at -40 to -60 mV and the larger inward current, seen at voltages negative to the K^+ equilibrium potential (E_K). This figure and figures 4 &5 also illustrate the effects of changing $[K^+]_o$ from 5 to 30 mmol/L on the reversal potential of this current. Note the positive shift that is evoked by 30 mmol/L $[K^+]_o$, as is predicted by the effects on E_K. To facilitate a quantification of I_{KIR} in the various vascular segments, the magnitude of the inward component of this current was assessed in both physiologic $[K^+]_o$. (5 mmol/L) and in 30 mmol/L $[K^+]_o$.

Figure 4 (top) depicts images of ILA segments isolated using our approach and images of ILA myocytes obtained from each segment. The lower panel of Figures 4A-4C depicts current tracings from myocytes isolated from ILA segments of 30, 50 and 70 µm diameter, respectively. Currents were recorded in 5 and 30 mmol/L $[K^+]_o$ and in the presence and absence of 100 µmol/L Ba^{2+}. Note that myocytes from the most distal ILA segment (30 µm, lower left) exhibited discernable Ba^{2+}-sensitive I_{KIR} even in 5 mmol/L $[K^+]_o$; whereas this current could not be detected in myocytes from the larger ILA segments under these conditions. In 30 mmol/L $[K^+]_o$, I_{KIR} was detected in both distal and intermediate (50 µm, lower center) ILA myocytes, but not in myocytes from the proximal (70 µm) ILA.

Mean data illustrating the current-voltage relationship of the Ba^{2+}-sensitive I_{KIR} are depicted in Figure 5A&B. Myocytes isolated from afferent arterioles (20 µm) and from 30 µm distal ILAs exhibited clearly discernible I_{KIR} in 5 mmol/L $[K^+]_o$ [-8±2 pA/pF, n=10, and -11±3 pA/pF, n=4, respectively, measured at -120 mV(Figure 5A)]. A smaller current was detected in myocytes from 40 µm ILA in 5 mmol/L $[K^+]_o$ (-4±2 pA/pF, n=6). In each case, I_{KIR} was enhanced ~5-fold in 30 mmol/L $[K^+]_o$. In 30 mmol/L $[K^+]_o$ (Figure 5B), myocytes from afferent arterioles, 30 µm and 40 µm ILAs exhibited I_{KIR} of -49±11, -46±17, and -20±6 pA/pF (at -120 mV), respectively. In 30 mmol/L $[K^+]_o$, I_{KIR} was also detected in myocytes from the 50 µm ILA segment (-8±4 pA/pF, at -120 mV, n=7). In this vessel, however, I_{KIR} was not discernable in 5 mmol/L $[K^+]_o$ (-0.7±0.6 pA/pF, n=7). By contrast, I_{KIR} was not detectable in the myocytes from the 70 µm ILA segment in either 5 or 30 mmol/L $[K^+]_o$ (4±3 pA/pF, n=5 and -2±2 pA/pF, n=6, respectively) . Thus while it is not possible to rule out a contribution of endothelial I_{KIR} in regard to the functional responses, the distribution of I_{KIR} in the myocytes from the vascular segments corresponds closely with functional responses to Ba^{2+} and elevated $[K^+]_o$.

The relationship between the density of I_{KIR} and vessel diameter is illustrated in Figure 5C. Note the inverse relationship between I_{KIR} density (measured at -120 mV in 30 mmol/L $[K^+]_o$) and vessel diameter (P<0.0001, correlation coefficient of -0.63). As shown in Figure 5D, while vessel diameter was related to current density, myocyte capacitance was not. As noted previously[4, 17], the myocytes of the afferent arteriole are quite small. Myocytes isolated from the ILA were of similarly size, ranging in capacitance from 6-8 pF.

Effects of Ba^{2+} on myogenic response

As discussed below, the distribution of I_{KIR} along the ILA corresponds to regional

differences in the functional properties of this vessel, including myogenic reactivity[8]. We therefore were interested in determining if blockade of I_{KIR}, by Ba^{2+}, might alter myogenic responses. Our previous attempt to address this issue was thwarted by the Ba^{2+}-induced vasoconstriction which prevented evaluations of myogenic reactivity in the presence of I_{KIR} blockade[3]. The protocol depicted in Figure 6A illustrates how we approached this issue in the present study. Myogenic reactivity was initially assessed (control), by recording steady-state diameters as renal arterial pressure was increased from 80 to 180 mmHg, in 20 mmHg steps (1 minute duration). As shown, this elicited a graded, pressure-dependent vasoconstriction. The kidneys were then treated with either 100 µmol/L $BaCl_2$ or 0.1 nmol/L angiotensin II, reducing diameters from 16.9±0.4 to 6.0±0.4 µm (n=5) and from 17.9±0.8 to 6.2±0.7 µm (n=5), respectively. Pinacidil (1 µmol/L) was then administered and increased diameters to 14.7±0.3 µm and 13.8±1.4 µm, respectively. Myogenic reactivity was then reassessed under these conditions. The results are summarized in Figure 6B. Diameters were normalized to the percent of the (basal) diameters at 80 mmHg to facilitate comparisons. In the angiotensin II group, basal diameters were 18.3±0.7 µm in controls and 13.4±1.4 µm following treatment with angiotensin II and pinacidil. Increasing perfusion pressures elicited similar decreases in diameters. At 180 mmHg, diameters were 8.0±0.6 µm (44±4 % of basal) in controls and 5.1±0.6 µm (38±5 % of basal) following treatment with angiotensin II and pinacidil (P=0.09). In the group treated with Ba^{2+}, basal diameters were 17.6±0.5 and 14.7±0.3 µm for controls and Ba^{2+} plus pinacidil. Myogenic responses were significantly reduced at all pressures. At 180 mmHg, diameters were 8.2±0.9 µm (46±4 % of basal) in controls and 12.2±0.9 µm (82±5 % of basal) following treatment with Ba^{2+} and pinacidil (P=0.002).

Discussion:

A characteristic of K_{IR} is that this channel is commonly seen in resistance vessels, but rarely observed in larger conduit arteries[25,30]. The diameter of the ILA decreases as the vessel courses from its origin at the arcuate artery to the superficial regions of the cortex. The properties of the ILA change from that of a conduit vessel near its origin, to that of a resistance vessel at its terminal segments. For example, the distal, but not proximal, segments exhibit myogenic vasoconstriction[8,28] and intraluminal pressures are reduced only at the terminal portions of the ILA[11,31]. In the present study, myocytes from the distal ILA exhibited large I_{KIR} and this ILA segment responded to manipulations known to alter I_{KIR}. This current was lacking in the proximal ILA; whereas the intermediate ILA exhibited mixed characteristics in regard to the function of K_{IR}, consistent with a transition between a conduit and resistance vessel at this segment.

Ba^{2+} blocks I_{KIR} in a relatively selective manner at concentrations below 100 μmol/L[25]. We previously reported that 30 μM Ba^{2+} elicited depolarization and vasoconstriction in the afferent arteriole[3]. Elevating $[K^+]_o$ (from 5 to 15 mmol/L) induced a hyperpolarization in afferent arterioles preconstricted with angiotensin II and elicited a vasodilation that is blocked by Ba^{2+}, but not by ouabain[3,4] . We also reported I_{KIR} in myocytes from afferent and efferent arterioles and both vessels expressed $K_{IR}2.1$[4], the isoform implicated in K^+-induced hyperpolarization in cerebral arteries[35]. Increases in $[K^+]_o$ shift the K^+ Nernst potential to more positive values, accounting for the observed depolarization and vasoconstriction. Modest increases in $[K^+]_o$ also increase the macroscopic current carried by K_{IR}[23] (online Fig.1S). The underlying mechanism involves a modification of the channel block by intracellular polyamine

and/or Mg^{2+}, which also accounts for the inward rectification[14,18]. Accordingly, an elevation in $[K^+]_o$ at the outer vestibule of the channel enhances the outward current. If I_{KIR} contributes to membrane potential, modest increases in $[K^+]_o$ evoke hyperpolarization and vasodilation in depolarized or pre-constricted vessels[4,10,12,13,24]. Otherwise this maneuver enhances depolarization, facilitating vasoconstriction. Elevated $[K^+]_o$ may also cause hyperpolarization by stimulating the electrogenic Na^+/K^+ ATPase[1,19,22]. These two mechanisms are distinguished by their sensitivities to Ba^{2+} and ouabain. We did not determine if the contribution of this latter mechanism varies along the ILA, but rather employed ouabain to rule out an involvement of Na^+/K^+ ATPase in the Ba^{2+}-sensitive K^+-induced vasodilation.

Ba^{2+} elicited a vasoconstriction in the distal ILA that was similar to that previously reported for the afferent arteriole (Figure 3). The distal ILA also dilated in response to elevated $[K^+]_o$ in a manner comparable to that of the afferent arteriole[3,4] (Figure 2C), although membrane potential responses were not obtained in the present study. The density of I_{KIR} , however, was similar in myocytes from afferent arterioles and 30 µm ILA in both 5 and 30 mmol/L $[K^+]_o$ (Figure 5). By contrast, the proximal ILA did not exhibit a detectable I_{KIR} and constricted, rather than dilated, in response to elevated $[K^+]_o$ (Figure 2B). While Ba^{2+}-induced vasoconstriction was not observed in either the intermediate or proximal ILA, the intermediate ILA exhibited a Ba^{2+}-sensitive K^+-induced vasodilatation. This vessel also exhibited a modest, but clearly detectable, I_{KIR} in 30 mmol/L $[K^+]_o$ (Figures 4&5). Consistent with the contractile responses, we observed that the magnitude of the Ba^{2+}-induced membrane depolarization correlated inversely with vessel diameters, providing the direct evidence for the important role of I_{KIR} in the control of membrane potential in the intact distal ILA.

Our analysis also demonstrated a significant inverse relationship between I_{KIR} density and vessel diameter (Figure 5). A similar relationship has been reported in the coronary and cerebral vasculatures[5,23,24]. Likewise, in the cremaster microcirculation, Ba^{2+}-induced vasoconstriction is limited to forth-order (~20 µm) arterioles[13]. Prior and coworkers had shown that I_{KIR} plays little role in the arcuate artery[22] , from which the proximal ILA originates. The present study demonstrates that K_{IR} current density increases with decreasing diameter along the ILA. In the most distal ILA segment, I_{KIR} is similar in magnitude to that of the afferent arteriole. K_{IR} is also expressed in the post-glomerular circulation and contributes to the regulation of membrane potential in the efferent arterioles[4] and in the vascular pericytes of the descending vasa recta[2].

The magnitude of I_{KIR} observed in renal microvascular myocytes merits comment. Myocytes from afferent arterioles and distal ILA exhibited I_{KIR} of -8 to -11 pA/pF in 5 mmol/L K^+ and -46±17 to -49±11 pA/pF in 30 mmol/L K^+ (measured at -120 mV), values relatively larger than those reported for other vascular myocytes[1, 21,23,34]. While the magnitude of I_{KIR} suggests a functional importance, the precise role of this current in the renal vasculature is not known. Alterations in I_{KIR}, mediated by protein kinase C (PKC) are implicated in vasoconstrictor responses[20,21,34] and this possibility requires additional study in the kidney. The significance of K^+-induced vasodilation, while appreciated in the cerebral and muscle circulations[7], is not clear in renal circulation. It has been suggested that an efflux of K^+ ions via endothelial K^+ channels, might constitute the long sought EDHF, via effects on K_{IR}[6]. This does not appear to be the case, however, for the afferent arteriole[32]. The findings presented in Figure 6 suggest an involvement of K_{IR} in the renal myogenic response, but the nature of this involvement is not apparent. For example, evidence suggests that I_{KIR} acts to amplify vascular electrical signals[26] and I_{KIR} could

play a permissive role in pressure-induced depolarization. K_{IR} is also required for the transmission of signals along the vasculature[9,26,27] and could be involved in distributing pressure signals within the renal circulation. The potential involvement of K_{IR} in the renal myogenic response is of considerable interest. In this regard, it is noteworthy that the distribution of I_{KIR} along the ILA corresponds closely to differences in myogenic reactivity along this vessel[8]. Clearly, further investigations are required to elucidate the precise physiologic roles of K_{IR} in the renal microcirculation.

Funding:

This work was supported by the Canadian Institutes for Health Research (MOP-14075); the Heart and Stroke Foundation of Alberta, Intuit and N.W.T. and the Alberta Heritage Foundation for Medical Research (AHFMR; 20090234; 20091182). SVS was supported by a visiting scientist grant from AHFMR and an international travel grant from the Royal Society. RL is an AHFMR Senior Investigator. LC was an AHFMR doctoral student and an Honorary Killam Memorial Scholar.

Conflict of Interest:

None declared.

References:

1. Burns WR, Cohen KD, Jackson WF. K^+-induced dilation of hamster cremasteric arterioles involves both the Na^+/K^+-ATPase and inward-rectifier K^+ channels. *Microcirculation* 2004;**11**:279-93.

2. Cao C, Goo JH, Lee-Kwon W, Pallone TL. Vasa recta pericytes express a strong inward rectifier K^+ conductance. *Am J Physiol Regul Integr Physiol* 2006;**290**:R1601-1607.

3. Chilton L, Loutzenhiser R. Functional evidence of inward rectifier potassium channel current in rat renal afferent arterioles. *Circ Res* 2001;**88**:152-158.

4. Chilton L, Loutzenhiser K, Morales E, Breaks J, Kargacin GJ, Loutzenhiser R. Inward rectifier K^+ currents and Kir2.1 expression in renal afferent and efferent arterioles. *J Am Soc Nephrol* 2008;**19**:69-76.

5. Edwards FR, Hirst GCS, Silverberg GD. Inward rectification in rat cerebral arterioles: involvement of potassium ions in autoregulation. *J Physiol* 1988;**404**:455-466.

6. Edwards G, Weston AH. Potassium and potassium clouds in endothelium-dependent hyperpolarizations. *Pharmacol Res* 2004;**49**:535–541.

7. Haddy FJ, Vanhoutte PM, Feletou M. Role of potassium in regulating blood flow and blood pressure. *Am J Physiol Regul Integr Comp Physiol* 2006;**290**:R546–R552.

8. Hayashi K, Epstein M, Loutzenhiser R. Enhanced myogenic responsiveness of renal interlobular arteries in spontaneously hypertensive rats. *Hypertension* 1992;**19**:153-160.

9. Jantzi MC, Brett SE, Jackson WF, Corteling R, Vigmond EJ, Welsh DG. Inward rectifying potassium channels facilitate cell-to-cell communication in hamster retractor muscle feed arteries. *Am J Physiol Heart Circ Physiol* 2006;**291**:H1319–H1328.

10. Jiang ZG, Si JQ, Lasarev MR, Nuttall AL. Two resting potential levels regulated by the inward-rectifier potassium channel in the guinea-pig spiral modiolar artery. *J Physiol* 2001;**537**:829-842.

11. Kâllskog Ô , Lindbom LO, Ulfendahl HR, Wolgast M. Hydrostatic pressures within the vascular structures of the rat kidney. *Pflügers Arch* 1979;**363**:205-210.

12. Knot HJ, Zimmermann PA, Nelson MT. Extracellular K^+-induced hyperpolarizations and dilatations of rat coronary and cerebral arteries involve inward rectifier K^+ channels. *J Physiol* 1996;**492**:419-430.

13. Loeb AL, Godény I, Longnecker DE. Functional evidence for inward-rectifier potassium channels in rat cremaster muscle arterioles. *Microvasc Res* 2000;**59**:1-6.

14. Lopatin AN, Nichols CG. $[K^+]$ dependence of polyamine-induced rectification in inward rectifier potassium channels (IRK1, Kir2.1). *J Gen Physiol* 1996;**108**:105-113.

15. Loutzenhiser R. In situ studies of renal arteriolar function using the in vitro perfused hydronephrotic rat kidney. *Int Rev Exp Pathol* 1996;**36**:145-160.

16. Loutzenhiser R, Bidani A, Chilton L. The renal myogenic response: kinetic attributes and physiologic role. *Circ Res* 2002;**90**:1316-1324.

17. Loutzenhiser K, Loutzenhiser, R. Angiotensin II-induced Ca^{2+} influx in renal afferent and efferent arterioles. Differing roles of voltage-gated and store-operated Ca^{2+} entry. *Circ Res* 2000;**87**:551-557.

18. Lopatin AN, Makhina EN, Nichols CG. Potassium channel block by cytoplasmic polyamines as the mechanism of intrinsic rectification. *Nature* 1994;**372**:366-369.

19. McCarron JG, Halpern W. Potassium dilates rat cerebral arteries by two independent

mechanisms. *Am J Physiol Heart Circ Physiol* 1990;**259**:H902-H908.

20. Park WS, Han J, Earm YE. Physiologic role of inward rectifier K^+ channels in vascular smooth muscle cells. *Pfügers Arch* 2008;**457**:137-147.

21. Park WS, Han J, Kim N, Youm JB, Joo H, Kim HK *et al*. Endothelin-1 inhibits inward rectifier K^+ channels in rabbit coronary arterial smooth muscle cells through protein kinase C. *J Cardiovasc Pharmacol* 2005;**46**:681-689.

22. Prior HM, Webster N, Quinn K, Beech DJ, Yates MS. K^+-induced dilation of a small renal artery: no role for the inward rectifier K^+ channel. *Cardiovasc Res* 1989;**37**:780-790.

23. Quayle JM, Dart C, Standin NB. The properties and distribution of inward rectifier potassium channels in pig coronary arterial smooth muscle. *J Physiol* 1996;**494**:715-726.

24. Quayle JM, McCarron JG, Brayden JE, Nelson MT. Inward rectifier K^+ currents in smooth muscle cells from rat resistance-sized cerebral arteries. *Am J Physiol Cell Physiol* 1993;**265**:C1363-C1370.

25. Quayle JM, Nelson MT, Standen NB. ATP-sensitive and inwardly rectifying potassium channels in smooth muscle. *Physiol Rev* 1997;**77**:1165-1232.

26. Rivers RJ, Hein TW, Zhang C, Kuo L. Activation of barium-sensitive inward rectifier potassium channels mediates remote dilation of coronary arterioles. *Circulation* 2001;**104**:1749–1753.

27. Smith PD, Brett SE, Luykenaar KD, Sandow SL, Marrelli SP, Vigmond EJ *et al*. KIR channels function as electrical amplifiers in rat vascular smooth muscle. *J Physiol* 2008;**586**:1147-1160.

28. Takenaka T, Suzuki H, Okada H, Hayashi K, Ozawa Y, Saruta T. Biophysical signals

underlying myogenic responses in rat interlobular artery. *Hypertension* 1998;**32**:1060-1065.

29. Tang L, Loutzenhiser K, Loutzenhiser R. Biphasic actions of prostaglandin E_2 on the renal afferent arteriole. *Circ Res* 2000;**86**:663-670.

30. Thorneloe KS, Nelson MT. Ion channels in smooth muscle: regulators of intracellular calcium and contractility. *Can J Physiol Pharmacol* 2005;**83**:215-242.

31. Tonder KJH, Aukland K. Interlobular arterial pressure in the rat kidney. *Renal Physiol* 1979;**2**:214-221.

32. Wang X, Loutzenhiser R. Determinants of renal microvascular response to acetylcholine: afferent and efferent arteriolar actions of EDHF. *Am J Physiol Renal Physiol* 2002;**282**:F124–F132.

33. Wang X, Takeya K, Aaronson PI, Loutzenhiser K, Loutzenhiser R. Effects of amiloride, benzamil, and alterations in extracellular Na^+ on the rat afferent arteriole and its myogenic response. *Am J Physiol Renal Physiol* 2008;**295**:F272-F282.

34. Wu BN, Luykenaar KD, Brayden JE, Giles WR, Corteling RL, Wiehler WB, Welsh DG. Hyposmotic challenge inhibits inward rectifying K^+ channel in cerebral arterial smooth muscle cells. *Am J Physiol Heart Circ Physiol* 2007;**292**:H1085–H1094.

35. Zaritsky JJ, Eckman DM, Wellman GC, Nelson MT, Schwarz TL. Targeted disruption of Kir2.1 and Kir2.2 genes reveals the essential role of the inwardly rectifying K^+ current in K^+-mediated vasodilation. *Circ Res* 2000;**87**:160–166.

Figure Legends:

Figure 1: K^+-induced dilation of distal interlobular artery (ILA). A: Tracing illustrating vasoconstriction elicited by elevating renal arterial pressure (RAP) from 80 to 160 mmHg and the vasodilation seen upon elevating $[K^+]_o$ from 5 to 15 mmol/L (KCl, black bar). Note that the vasoconstriction was restored when $[K^+]_o$ was returned to 5 mmol/L. B: Mean data comparing distal ILA response to elevated $[K^+]_o$ in the presence of vasoconstriction elicited by elevated pressure (n=26), angiotensin II (Ang II, n=4), 100 µmol/L Ba^{2+} (n=6) and 3 mmol/L ouabain (n=11, 10 µmol/L propranolol and phentolamine present). Vasodilation was blocked by Ba^{2+}, but not by ouabain.

Figure 2: Responses of intermediate and proximal ILA to elevated $[K^+]_o$. A: Intermediate ILA pre-constricted with angiotensin II (Ang II, grey bars) exhibited significant vasodilation when $[K^+]_o$ was elevated from 5 to 15 mmol/L (black bars). This response was preserved in the presence of ouabain (3 mmol/L, with 10 µmol/L propranolol and phentolamine present (n=6), but was prevented by addition of Ba^{2+} (100 µmol/L). B: Proximal ILA did not dilate in response to increased $[K^+]_o$, but rather exhibited an increased vasoconstriction (n=6). C: Comparison of responses of distal, intermediate and proximal responses, observed during Ang II-induced vasoconstriction. For comparative purposes previously published data[5] for the afferent arteriole* under the same experimental conditions are shown.

Figure 3: Segment-specific effects of Ba^{2+} on diameters (A&B, perfused kidney model) and membrane potential (C&D, isolated vessels). A: Ba^{2+} (30 and 100 µmol/L) did not cause vasoconstriction in proximal (n=9) or intermediate (n=5) ILA segments, but induced significant vasoconstriction in the distal ILA (* indicates $P<0.03$ versus basal diameter, n=6). B: Comparison of Ba^{2+} responses of ILA segments. For comparative purposes, previously published data[3] for the afferent arteriole are also shown. C: Tracings illustrating effects of Ba^{2+} on membrane potential of isolated renal microvessels. D: Relationship between vessel diameter and magnitude of Ba^{2+}-induced depolarization in 9 isolated afferent arterioles and ILA segments.

Figure 4. Top panel depicts examples of ILA segments and myocytes obtained using the gel-perfusion technique (calibration bar = 30 µm). Bottom panel depicts tracings of voltage ramp protocol and current recordings measured in 5 mmol/L and 30 mmol/L $[K^+]_o$ in the absence and presence of 100 µmol/L Ba^{2+}. The proximal (30 µm) ILA myocyte exhibited a significant Ba^{2+}-sensitive inward current (I_{KIR}) in 5 mmol/L $[K^+]_o$; whereas I_{KIR} could not be detected in myocytes from larger ILA under this condition. In 30 mmol/L $[K^+]_o$, a substantially larger I_{KIR} is seen in the distal ILA myocyte (A) and I_{KIR} could also be detected in the intermediate (50 µm) ILA myocyte (B), but not in the proximal (70 µm) ILA myocyte (C) ILA. Trace "WO" (wash out, A) shows reversibility of Ba^{2+} effect.

Figure 5. A&B: Current/voltage relationships for Ba^{2+}-sensitive (I_{KIR}) densities in the myocytes isolated from afferent arterioles (AA) and ILA segments. I_{KIR} obtained by subtracting residual currents in presence of 100 µmol/L Ba^{2+} from basal currents in either 5 (A) or 30 (B) mmol/L

$[K^+]_o$. Numbers in parentheses correspond to the number of myocytes in each group. C: Relationship between I_{KIR} (measured at -120 mV) and the vessel diameter. Note significant correlation (R = -0.63, $P<0.0001$). The dashed lines represent 95% confidence interval. D: I_{KIR} density was independent on the size of the myocyte, as estimated by cell capacitance.

Figure 6. A: Effect of Ba^{2+} on myogenic response. Myogenic responses were initially assessed under control conditions for both types of treatment (filled symbols). The kidneys were then exposed to similar levels of vasoconstriction induced by angiotensin II (Ang II, 0.1 nmol/L, circles) or Ba^{2+} (100 µmol/L, squares). The K_{ATP} opener pinacidil (1.0 µmol/L) was then administered to partially restore basal diameters and allow myogenic reactivity to be reassessed. B: Comparisons of the myogenic responses in angiotensin II (open circles) or Ba^{2+} (open squares) to the corresponding controls (filled symbols). Diameters were normalized to percent of basal diameter (80 mmHg). *$P<0.05$ vs control.

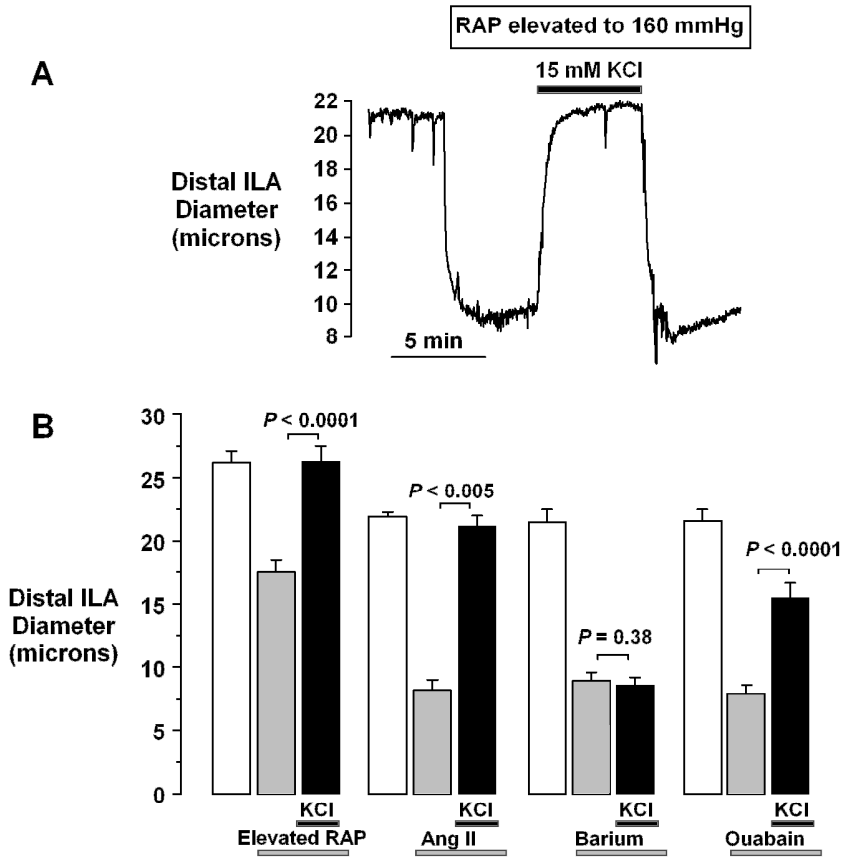

Figure 1

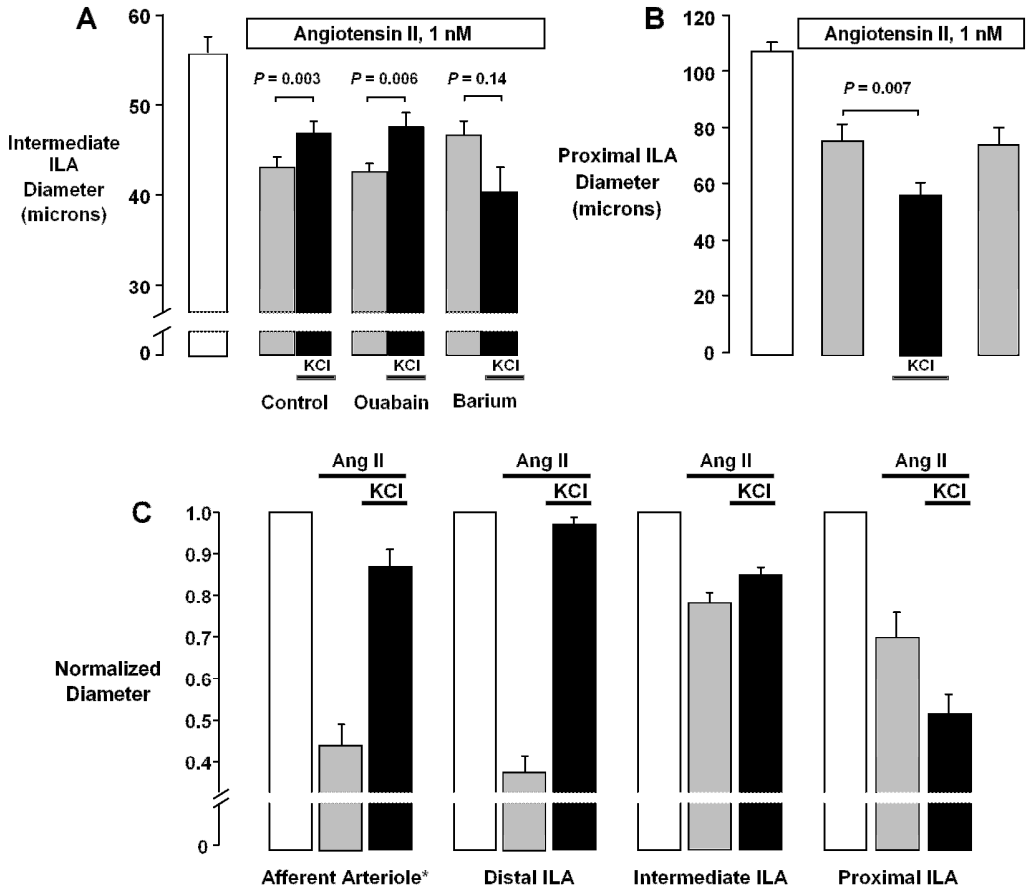

Figure 2

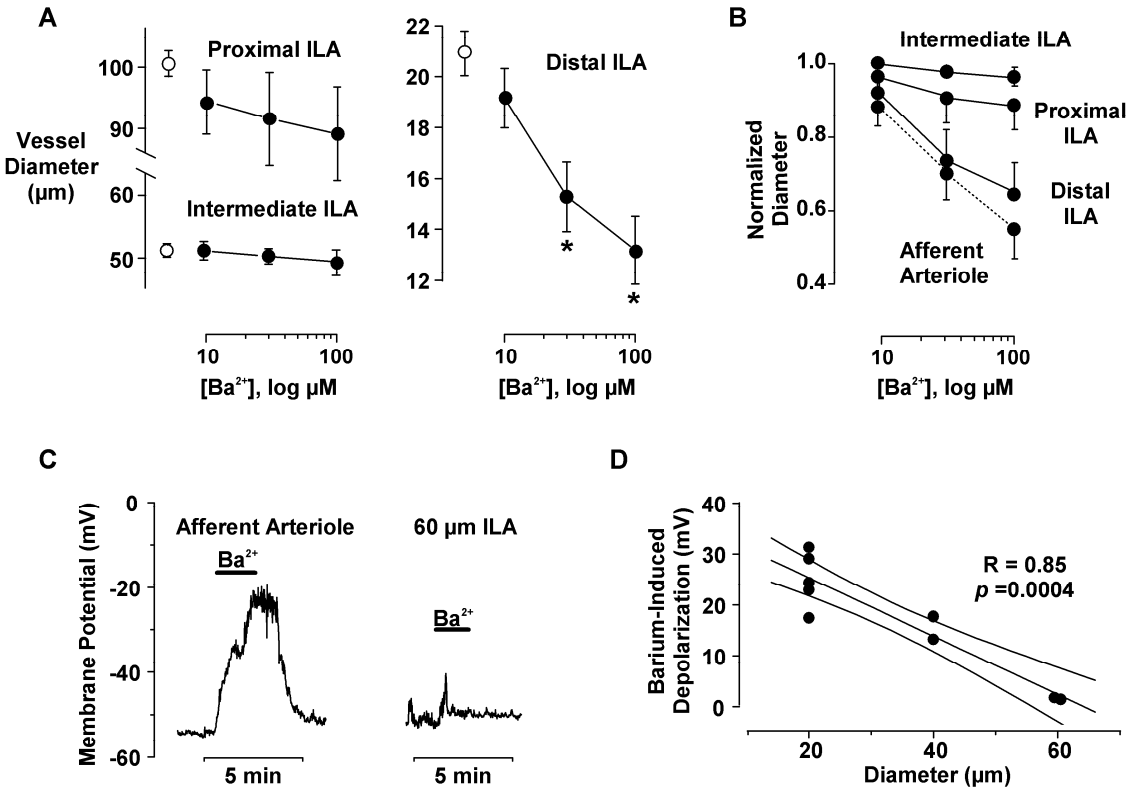

Figure 3

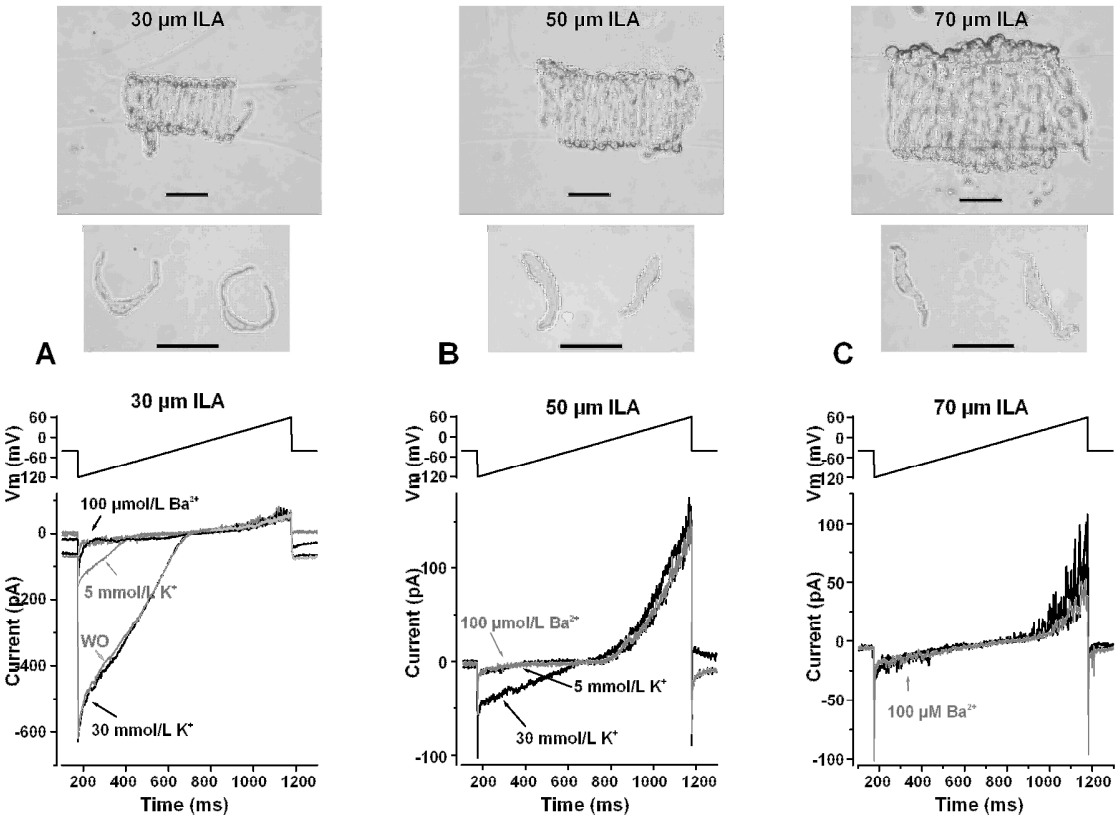

Figure 4

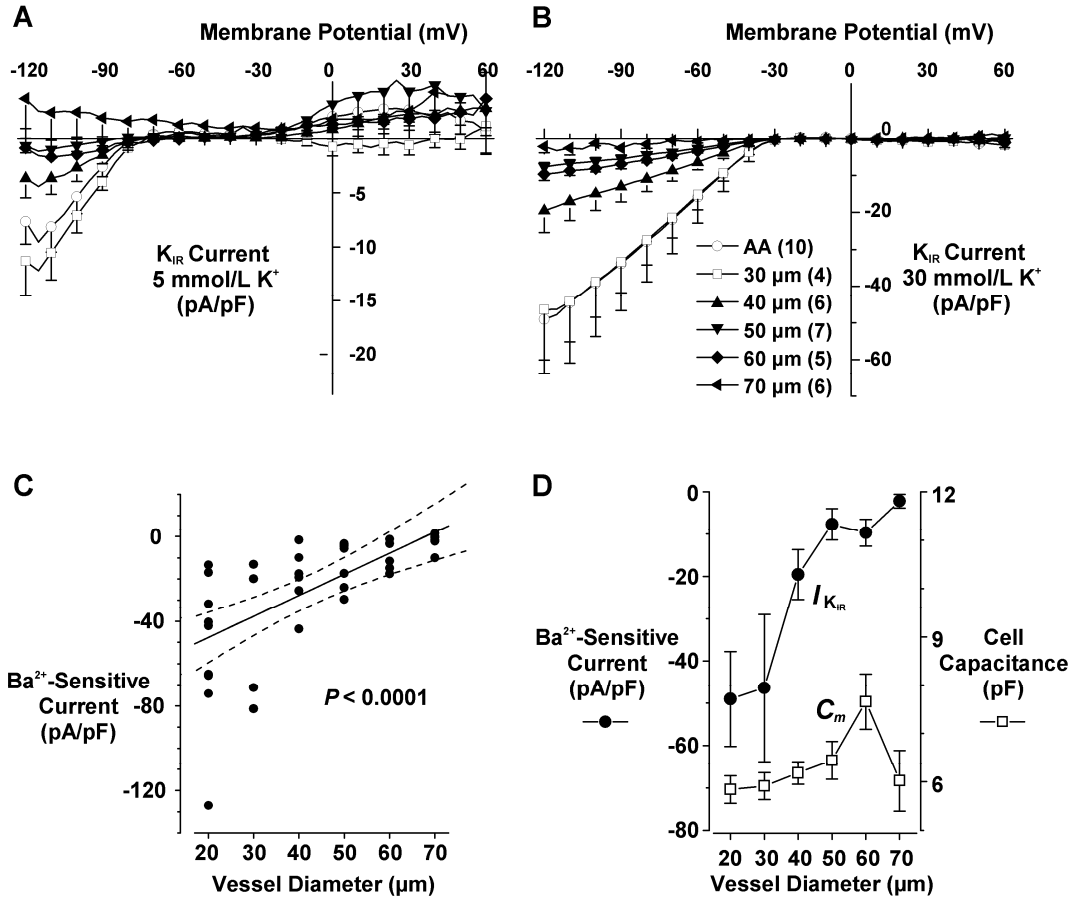

Figure 5

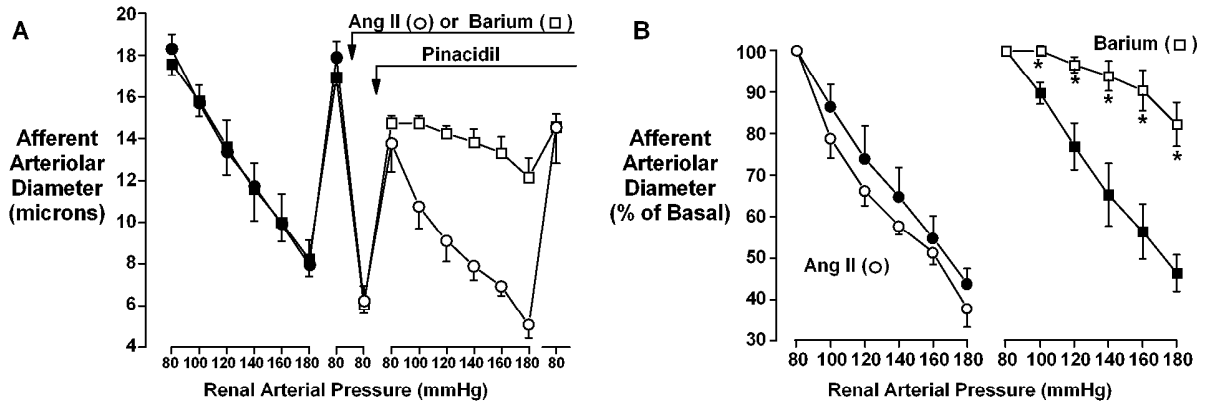

Figure 6